Current Biology 23, 2423–2429, December 2, 2013 ©2013 Elsevier Ltd All rights reserved http://dx.doi.org/10.1016/j.cub.2013.10.023

Report

Antagonistic Spindle Motors and MAPs Regulate Metaphase Spindle Length and Chromosome Segregation

Viktoriya Syrovatkina,[1,4] Chuanhai Fu,[1,2,4] and Phong T. Tran[1,3,*]
[1]Department of Cell and Developmental Biology, University of Pennsylvania, Philadelphia, PA 19104, USA
[2]Department of Biochemistry, The University of Hong Kong, Pok Fu Lam, Hong Kong, China
[3]Institut Curie, CNRS UMR144, 75005 Paris, France

Summary

Metaphase describes a phase of mitosis where chromosomes are attached and oriented on the bipolar spindle for subsequent segregation at anaphase. In diverse cell types, the metaphase spindle is maintained at characteristic constant length [1–3]. Metaphase spindle length is proposed to be regulated by a balance of pushing and pulling forces generated by distinct sets of spindle microtubules (MTs) and their interactions with motors and MT-associated proteins (MAPs). Spindle length is further proposed to be important for chromosome segregation fidelity, as cells with shorter- or longer-than-normal metaphase spindles, generated through deletion or inhibition of individual mitotic motors or MAPs, showed chromosome segregation defects. To test the force-balance model of spindle length control and its effect on chromosome segregation, we applied fast microfluidic temperature control with live-cell imaging to monitor the effect of deleting or switching off different combinations of antagonistic force contributors in the fission yeast metaphase spindle. We show that the spindle midzone proteins kinesin-5 cut7p and MT bundler ase1p contribute to outward-pushing forces and that the spindle kinetochore proteins kinesin-8 klp5/6p and dam1p contribute to inward-pulling forces. Removing these proteins individually led to aberrant metaphase spindle length and chromosome segregation defects. Removing these proteins in antagonistic combination rescued the defective spindle length and in some combinations also partially rescued chromosome segregation defects.

Results and Discussion

In diverse cell types, the metaphase spindle maintains a characteristic steady-state constant length [1–3], which is thought to be important for ensuring correct chromosome-to-microtubule (MT) attachment prior to anaphase. It is proposed that a balance of antagonistic forces produced by motors and MT-associated proteins (MAPs) located at the spindle midzone, the kinetochore, and/or astral MTs is required to maintain the constant metaphase spindle length [1–3]. However, the force-balance model has never been tested in a live-cell manner. In rare occasions of removal of antagonistic forces, e.g., double deletion of antagonistic motors, the metaphase spindle length appeared rescued [4–7], but its subsequent effect on chromosome segregation was not known.

We present here a live-cell study using the simple fission yeast *Schizosaccharomyces pombe*, combined with fast microfluidic temperature control for inactivating thermosensitive genes, effectively tuning protein functions on/off rapidly during mitosis, to directly test the force-balance model and determine its consequences on chromosome segregation. Fission yeast exhibits all the phases of mitosis seen in mammalian cells [8]. However, unlike mammalian cells, the number of motors and MAPs implicated in spindle dynamics in fission yeast are fewer [9]. Thus, mechanisms of fission yeast spindle length regulation may be viewed as "core" conserved mechanisms through evolution.

Motors and MAPs Control the Steady-State Constant Metaphase Spindle Length

We reasoned that forces contributing to the metaphase spindle length maintenance would come from motors and MAPs [1–3]. To define a set of antagonistic motors and MAPs regulating spindle length, we performed a targeted deletion or inactivation screen of the fission yeast motors and selective MAPs known to have spindle length defects. We used the degradation of cyclin B (cdc13p-GFP) as a proxy for metaphase-to-anaphase transition (Figure 1A) [10, 11] and defined the final metaphase spindle length as the length immediately before the disappearance of cdc13p-GFP from the spindle. Our screen identified the kinetochore proteins heterodimer kinesin-8 klp5/6p and the MT coupler dam1p as the major contributors to the inward-pulling force on the spindle, as their individual deletion resulted in longer metaphase spindles compared to wild-type (Figure 1B), consistent with previous findings [12, 13]. Kinesin-8 klp5/6p is a MT plus-end depolymerase that converts MT depolymerization to cargo movement [14, 15]. Similarly, dam1p is a MAP that binds processively to MT and converts MT depolymerization to cargo movement [16, 17]. Thus, Klp5/6p can be viewed as an active force transducer and dam1p can be viewed as a passive force transducer, both converting MT depolymerization into the inward-pulling force experienced by the spindle. We also identified the spindle midzone bundler MAP ase1p as the major contributor to the outward-pushing force on the spindle, as its deletion resulted in shorter metaphase spindles compared to wild-type (Figure 1B), consistent with previous findings [18, 19]. As a MT bundler of defined angular polarity [20], ase1p can be viewed as a force resistor, resisting the inward force due to klp5/6p and dam1p. Finally, kinesin-14 pkl1p also appeared to play a major role in spindle length control, as its deletion resulted in shorter metaphase spindles compared to wild-type (Figure 1B). However, its reported localization at the spindle pole body [7] and its role in focusing MTs at the spindle poles [21, 22] suggest that it does not directly contribute to the pulling or pushing forces for spindle length control but instead plays a role in spindle formation itself. Indeed, we observed a high frequency of MT protrusions from the spindle poles in pkl1Δ cells: ~50% of spindles have protrusion in pkl1Δ cells, compared to zero in wild-type cells (see Figures S1A and S1B available online), indicative of

[4]These authors contributed equally to this work
*Correspondence: tranp@mail.med.upenn.edu

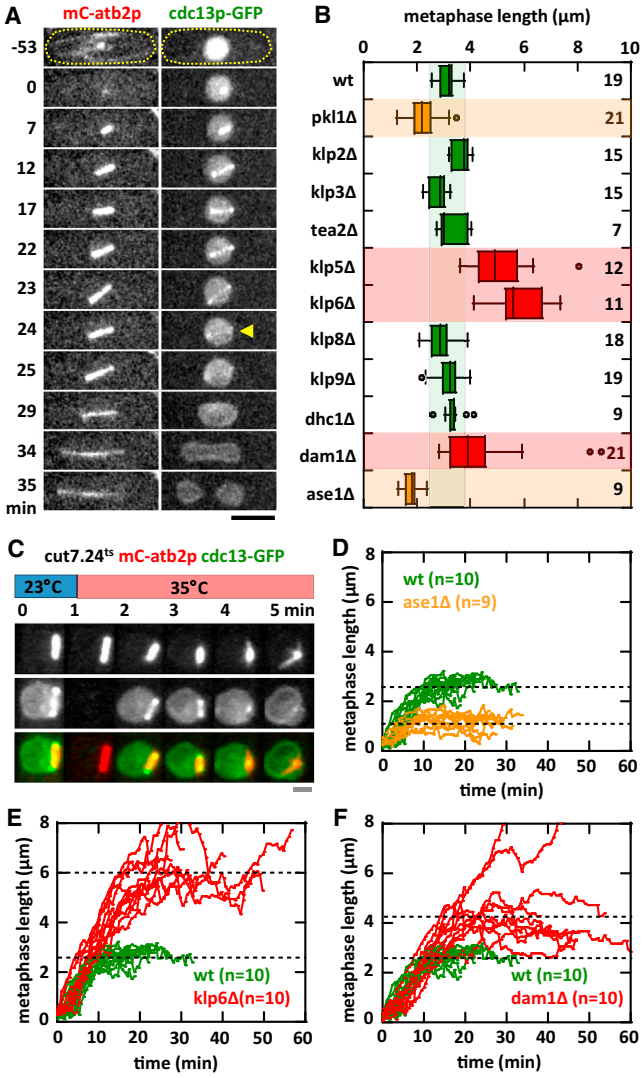

Figure 1. Motors and MAPs Contribute to Metaphase Spindle Length Force-Balance Mechanism

(A) Time-lapse images of a wild-type cell expressing mCherry-atb2p (tubulin) and cdc13p-GFP (cyclin) through mitosis. cdc13p is degraded from the spindle at the metaphase/anaphase transition (yellow arrow), marking precisely the final metaphase spindle length. The cdc13p-GFP marker is used in the screen for motors and MAPs affecting metaphase spindle length (see Figure 1B). Scale bar represents 5 μm.

(B) Targeted screen of fission yeast motors and selective MAPs for defects in metaphase spindle length at room temperature (23°C). The box plot shows spindle lengths: wild-type (3.1 ± 0.3 μm), pkl1Δ (2.0 ± 0.4 μm, $p < 10^{-4}$), klp2Δ (3.6 ± 0.3 μm, $p < 10^{-4}$), klp3Δ (2.8 ± 0.4 μm, p = 0.1), tea2Δ (3.3 ± 0.5 μm, p = 0.3), klp5Δ (5.3 ± 1.2 μm, $p < 10^{-4}$), klp6Δ (6.3 ± 1.6 μm, $p < 10^{-4}$), klp8Δ (2.9 ± 0.5 μm, p = 0.4), klp9Δ (3.4 ± 0.4 μm, p = 0.6), dhcΔ (3.4 ± 0.4 μm, p = 0.1), dam1Δ (4.4 ± 1.6 μm, $p < 10^{-2}$), and ase1Δ (1.8 ± 0.3 μm, $p < 10^{-7}$).

(C) Temperature-shift experiment of kinesin-5 cut7.24^{ts} cells expressing mCherry-atb2p and cdc13p-GFP. Within 1 min of shifting to the nonpermissive temperature of 35°C, the metaphase spindle exhibits spindle shortening and collapse, ultimately becoming a monopolar spindle. Note that the blank image at time 1 min in the cdc13p-GFP channel was due to thermal expansion of the coverslip causing an out-of-focus image, which was corrected in subsequent frames. Scale bar represents 1 μm.

(D) Comparative plot of spindle length versus time of wild-type (green) and ase1Δ (orange) cells. Pole-to-pole distances measured from prophase to the metaphase-anaphase transition are shown. Wild-type metaphase spindles plateau at ~3 μm length. In contrast, ase1Δ metaphase spindles plateau at ~2 μm length.

spindle malformation. We thus exclude pkl1p from the current analysis. Although numerous motors and MAPs have been reported to play a role in metaphase spindle length regulation [4, 6], for clarity, we focus on the motors and MAPs that have the strongest measureable defects in spindle lengths and localize only to the kinetochores or the spindle midzone.

Kinesin-5 cut7p is reported to play a role in biopolar spindle formation, by organizing and sliding apart antiparallel MTs from opposite poles [23]. cut7p is essential, and a conditional temperature-sensitive strain was isolated previously [23]. We used a microfluidic fast temperature-control device created in our lab [24] to inactivate the temperature-sensitive cut7.24^{ts} strain precisely at metaphase (Figure 1C). Upon inactivation of cut7p at the nonpermissive 35°C, the metaphase spindle immediately shortened until the spindle became a focused monopolar structure (Figure 1C). This is consistent with cut7p being the major contributor to the outward-pushing force. Thus, cut7p can be viewed as an active force producer, sliding interpolar MTs apart as the outward-pushing force experienced by the spindle.

Interestingly, in *C. elegans* and mammalian somatic cells, kinesin-5 Eg5 is not needed for the maintenance of metaphase spindle length [25–27]. In mammals, highly dynamic interpolar MTs can compensate for the absence of Eg5 [28], and in *C. elegans*, the relatively more robust astral MTs, compared to the smaller interpolar MTs, can produce pulling force on the spindle and compensate for the absence of Eg5 [27]. In comparison, fission yeast has no astral MTs during metaphase and does not have highly dynamic and robust interpolar MTs. Therefore, cut7p becomes indispensable for spindle length maintenance in fission yeast.

We next monitored spindle elongation dynamics to determine how the new steady-state spindle length is achieved. As inactivation of cut7p completely shortened the metaphase spindle (Figures 1C and 2A), we examined ase1Δ, klp6Δ, and dam1Δ mutants. The spindle of wild-type cells typically elongates at 0.23 ± 0.02 μm/min during prophase to reach a steady-state metaphase length of 3.10 ± 0.34 μm, with duration of prophase-metaphase of 22 ± 5 min (Figures 1D–1F; Figures S1C and S1D). In contrast, ase1Δ elongates at 0.10 ± 0.03 μm/min and has metaphase length of 1.82 ± 0.33 μm and prophase-metaphase duration of 28 ± 3 min; klp6Δ elongates at 0.32 ± 0.04 μm/min and has metaphase length of 6.33 ± 1.60 μm and prophase-metaphase duration of 38 ± 11 min; and dam1Δ elongates at 0.21 ± 0.07 μm/min and has metaphase length of 4.41 ± 1.62 μm and prophase-metaphase duration of 52 ± 13 min (Figures 1D–1F; Figures S1C and S1D).

We stress that changes in spindle length are likely due primarily to the force contributors and not to the activation of the spindle assembly checkpoint (SAC) [29–32], which would be expected to prolong the prophase-metaphase duration and lead to changes in spindle length. In the absence of mad2p, a major SAC protein monitoring kinetochore-to-MT attachment [29–32], metaphase spindle lengths in the double deletions klp5Δ:mad2Δ and dam1Δ:mad2Δ remained similar to that of klp5Δ and dam1Δ alone, respectively (Figure S1E),

(E) Comparative plot of spindle length versus time of wild-type (green) and klp6Δ (red) cells. In contrast to wild-type, klp6Δ metaphase spindles plateau at ~6 μm length.

(F) Comparative plot of spindle length versus time of wild-type (green) and dam1Δ (red) cells. In contrast to wild-type, dam1Δ metaphase spindles plateau at ~4 μm length.

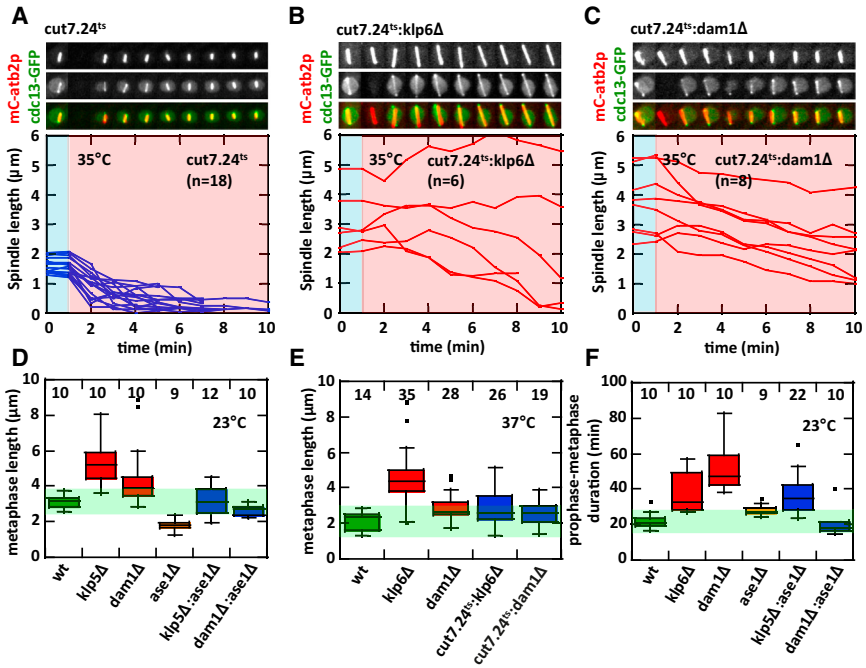

Figure 2. Removing Antagonistic Spindle Forces Rescues Metaphase Spindle Length Defects

(A) Temperature-shift experiment of cut7.24^{ts} cells expressing mCherry-atb2p and cdc13p-GFP. The accompanying plot of spindle length versus time shows that all cut7.24^{ts} metaphase spindles shorten and collapse within ~3–4 min at the nonpermissive temperature of 35°C.

(B) Temperature-shift experiment of cut7.24^{ts}:klp6Δ double-mutant cells. The double-mutant cells do not exhibit the fast spindle collapse seen in cut7.24^{ts} alone (see Figure 2A). The metaphase spindles maintain transiently stable lengths during the 10 min of observation at the nonpermissive temperature.

(C) Temperature-shift experiment of cut7.24^{ts}:dam1Δ double-mutant cells. The double-mutant cells do not exhibit the fast spindle collapse seen in cut7.24^{ts} alone. The metaphase spindles slowly shorten during the 10 min of observation at the nonpermissive temperature.

(D) Box plot shows metaphase spindle lengths measured at 23°C. Individual mutants have defective spindle length. Metaphase spindle lengths for wild-type, klp5Δ, dam1Δ, and ase1Δ are reported in Figure 1B. In contrast, antagonistic double mutants rescue the spindle length defects of the single mutants. Metaphase spindle length of klp5Δ:ase1Δ (3.2 ± 0.8 μm) is similar to wild-type ($p = 0.8$), and dam1Δ:ase1Δ (2.6 ± 0.3 μm) is between dam1Δ ($p < 10^{-4}$) and ase1Δ ($p < 10^{-4}$).

(E) Box plot shows metaphase spindle lengths measured at 37°C. Individual mutants have defective spindle lengths. Metaphase spindle lengths for wild-type (2.2 ± 0.5 μm), cut7.24^{ts} (1.5 ± 0.4 μm, $p < 0.004$), klp6Δ (4.6 ± 1.6 μm, $p < 10^{-10}$), and dam1Δ (2.9 ± 0.7 μm, $p < 10^{-3}$) are shown. In contrast, antagonistic double mutants rescue the spindle length defects of the single mutants. Metaphase spindle length of cut7.24^{ts}:klp6Δ (2.9 ± 1.0 μm) is between cut7.24^{ts} ($p < 10^{-5}$) and klp6Δ ($p < 10^{-5}$), and cut7.24^{ts}:dam1Δ (2.7 ± 0.7 μm) is between cut7.24^{ts} ($p < 10^{-4}$) and dam1Δ ($p = 0.2$).

(F) Box plot shows prophase-metaphase duration measured at 23°C. Individual mutants have prolonged prophase-metaphase durations. Durations are as follows: wild-type (22 ± 5 min), klp6Δ (38 ± 11 min, $p < 0.002$), dam1Δ (52 ± 13 min, $p < 10^{-4}$), and ase1Δ (28 ± 3 min, $p < 0.007$). In contrast, some antagonistic double mutants rescue prophase-metaphase duration defects of the single mutants. Duration of dam1Δ:ase1Δ (21 ± 7 min) is similar to wild-type ($p = 0.5$), and klp5Δ:ase1Δ (37 ± 11 min) is similar to klp6Δ ($p = 0.8$).

while the prophase-metaphase duration of the double mutants is similar to that of wild-type (Figure S1F). We conclude that, consistent with the force-balance model, removing individual contributors of force results in enhanced antagonistic effect from the remaining force contributors, which leads to a new steady-state metaphase spindle length.

Removal of Antagonistic Spindle Forces Can Rescue Metaphase Spindle Length Defects

Pushing and pulling can be viewed as antagonistic forces controlling the steady-state metaphase spindle length. To test whether removal of antagonist force contributors can restore or rescue the metaphase spindle length to that of wild-type, we observed metaphase spindle length upon deletion and/or inactivation of antagonistic force contributors. As shown, inactivation of cut7p at 35°C with the fast microfluidic temperature-control device led to an immediate decrease in metaphase spindle length (Figures 1C and 2A). The decrease was relatively quick, occurring over durations of ~3–4 min (Figure 2A). The quick spindle shrinkage was the result of the inactivation of cut7.24^{ts} while both klp5/6p and dam1p were still present. In klp6Δ cells, where metaphase spindles were longer than wild-type due to the removal of the inward-pulling force contributor klp6p (Figures 1B and 2B), inactivation of cut7p did not immediately lead to spindle shrinkage (Figure 2B). Instead, the majority of the cut7.24^{ts}:klp6Δ spindles slowly decreased in length over the 10 min observation duration, and some even maintained the same length or slightly increased in length (Figure 2B). Our interpretation is that in the absence of klp6Δ, dam1p is still at the kinetochore to capture MTs. Further, dam1p is passive, waiting for a MT depolymerization event to manifest the pulling force [16, 17]. If no MT depolymerization occurs, no pulling force would be possible, resulting in no spindle length decrease or even in an increase in spindle length in the short term (~5 min duration). In the long-term, all MTs will tend to depolymerize, and dam1p would then act to pull the spindle inward slowly [16, 17]. A similarly slow spindle length decrease is also observed in the dam1Δ cells when cut7p is inactivated (Figure 2C). However, all cut7.24^{ts}:dam1Δ spindles showed persistent slow spindle length decrease. Our interpretation is that in the absence of dam1Δ, klp6p at the kinetochore can still capture MTs and persistently promote MT depolymerization, resulting in sustained slow spindle shrinkage [14, 15]. Thus, force balance is a tug-of-war between cut7p and ase1p against klp5/6p and dam1p. This model predicts that the triple removal of cut7p, klp5/6p, and dam1p would remove both inward and outward forces, leading to a static constant-length metaphase spindle. The double deletion dam1Δ:klp5Δ is lethal [33]. However, the temperature-sensitive double mutant dam1-A8:klp5Δ is viable (but very sick) at room temperature and lethal at the nonpermissive 37°C [33]. Our numerous attempts to construct the triple deletion-inactivation mutant cut7.24^{ts}:dam1-A8:klp5Δ proved unsuccessful, most likely because dam1-A8:klp5Δ itself is very sick, even at permissive temperature [33]. Nevertheless, the dam1-A8:klp5Δ double mutant exhibits longer metaphase spindles compared to the individual mutants dam1Δ and klp5Δ or to the wild-type cells

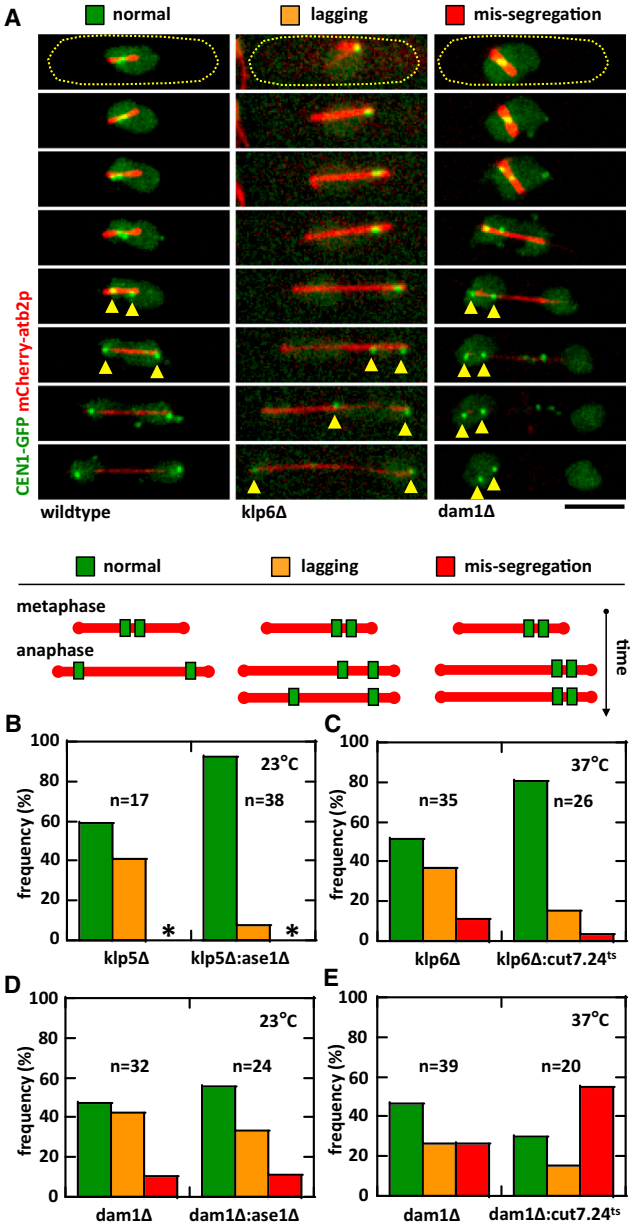

Figure 3. Rescuing Metaphase Spindle Length Defects Partially Rescues Chromosome Segregation Defects

(A) Time-lapse images of mitotic cells expressing mCherry-atb2p (tubulin) and CEN1-GFP (centromere of chromosome 1). We defined the behavior of chromosomes as: normal, sister centromeres separate equally to daughter cells at anaphase (green); lagging, sister centromeres show delayed separation to daughter cells at anaphase (orange); and missegregation, sister centromeres stay in one daughter cell at the completion of mitosis (red).

(B) Plot shows frequency comparison of chromosome behavior between klp5Δ and klp5Δ:ase1Δ at 23°C. No chromosome missegregation is observed for these strains (asterisk). The klp5Δ:ase1Δ strain shows ~90% normal chromosome segregation compared to ~60% for klp5Δ alone ($p < 10^{-34}$). Note that wild-type cells have 100% normal chromosome segregation.

(C) Plot shows frequency comparison of chromosome behavior between klp6Δ and cut7.24ts:klp6Δ at 37°C. The cut7.24^{ts}:klp6Δ strain shows ~80% normal chromosome segregation compared to ~50% for klp6Δ alone ($p < 10^{-9}$).

(D) Plot shows frequency comparison of chromosome behavior between dam1Δ and dam1Δ:ase1Δ cells at 23°C. No significant changes in the behavior of chromosomes was observed in the double mutant compared to the single mutant ($p = 0.2$).

(E) Plot shows frequency comparison of chromosome behavior between dam1Δ and dam1Δ:cut7.24^{ts} at 37°C. Indeed, the dam1Δ:cut7.24^{ts} strain shows ~55% of missegregation compared to ~25% for dam1Δ alone ($p < 10^{-9}$).

(Figures S2B and S2C), consistent with the tug-of-war analogy. In the course of this study, we also discovered that temperature sensitivity is tenuous. It is known that different temperature-sensitive alleles of cut7^{+} have different inactivation penetration, e.g., cut7.24^{ts} is lethal but cut7.21^{ts} and cut7.23^{ts} are not lethal (but are very sick) at the nonpermissive temperature [7]. Furthermore, we find that the allele cut7.24^{ts}, when tagged with GFP, is no longer lethal at 37°C (Figure S2A), presumably because GFP confers added stability to the cut7.24^{ts} gene product. This implies that creating a fast-acting, strongly penetrant, temperature-sensitive mutant allele requires some serendipity.

We next measured the metaphase spindle lengths after the removal of different combinations of antagonist forces. We found that for all combinations of double deletion, the removal of antagonist forces led to metaphase spindle lengths similar to wild-type and different from individual deletion (Figure 2D). Indeed, klp5Δ:ase1Δ has a metaphase length of 3.17 ± 0.78 μm and dam1Δ:ase1Δ has a metaphase length of 2.65 ± 0.31 μm, values significantly different from individual deletions (Figure 2D). Interestingly, only the double deletion dam1Δ:ase1Δ appeared to rescue the prophase-metaphase duration (Figure 2F), but klp5Δ:ase1Δ showed prophase-metaphase delay similar to individual klp5Δ deletion. Furthermore, while metaphase spindle length and some prophase-metaphase durations appeared rescued in the double deletion, the prophase velocities were only partially rescued for dam1Δ:ase1Δ (Figures S2E and S2F) and not rescued at all for klp5Δ:ase1Δ (Figures S2D and S2F). At the nonpermissive temperature of 35°C, cut7.24^{ts}:klp6Δ had a metaphase length of 2.88 ± 1.04 μm and cut7.24^{ts}:dam1Δ had a metaphase length of 2.65 ± 0.68 μm, values closer to the wild-type 2.16 ± 0.50 μm than the individual deletion or inhibition (Figure 2E). These results are consistent with the role of cut7p as an active pushing-force producer, klp5/6p as an active pulling-force transducer, dam1p as a passive pulling-force transducer, and ase1p as a passive pulling-force resistor. Antagonism between cut7p and ase1p against klp5/6p and dam1p results in a steady-state spindle length. Removal of any single or combination of force contributors will result in a new steady-state length. The transition from one length to a new length can be smooth (stable) or not smooth (unstable), depending on the state of antagonism. In general, active-active antagonism, such as found in dam1Δ:ase1Δ, tends to produce a stable transition, represented by the smooth length-versus-time trace (Figure S2E). In contrast, an active-passive antagonism, such as found in klp5Δ:ase1Δ, tends to produce an unstable transition, represented by strong variations in the length-versus-time trace (Figure S2D). Furthermore, stable spindle transition, such as found in dam1Δ:ase1Δ (Figure S2E), may enable efficient kinetochore-to-MT attachment, which will result in seemingly normal (or rescued) prophase-metaphase duration (Figure 2F). In contrast, unstable spindle transition, such as found in klp5Δ:ase1Δ (Figure S2D), will be inefficient at kinetochore-to-MT attachment, which will result in a higher prophase-metaphase duration (Figure 2F), likely due to the activation of the SAC.

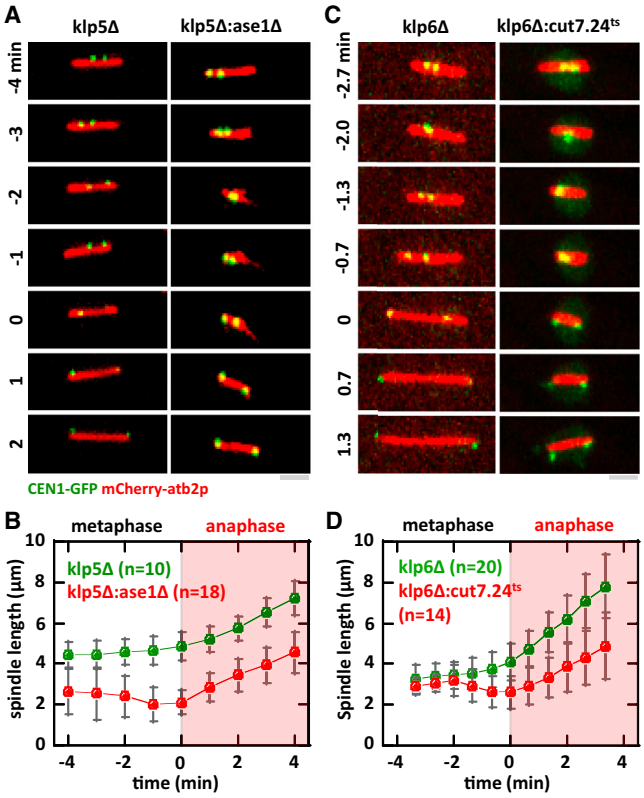

Figure 4. Transient Abrupt Metaphase Spindle Length Decrease Precedes Proper Chromosome Segregation

(A) Time-lapse images of klp5Δ and klp5Δ:ase1Δ mitotic cells expressing mCherry-atb2p and CEN1-GFP at 23°C. Time 0 represents the transition from metaphase to anaphase A where sister kinetochores are observed to separate to opposite poles. Whereas the metaphase spindle exhibits sustained elongation during the metaphase/anaphase transition in klp5Δ cells, klp5Δ:ase1Δ cells show transient spindle shrinkage prior to the metaphase/anaphase transition. Scale bar represents 1 μm.

(B) Comparative spindle length versus time plot of klp5Δ (green) and klp5Δ:ase1Δ (red) cells. Pole-to-pole distance was measured 4 min before and 4 min after cells exhibited kinetochore separation to opposite poles. At −2 min, the spindle length of the double mutant exhibits a transient shrinkage.

(C) Time-lapse images of klp6Δ and klp6Δ:cut7.24^{ts} mitotic cells expressing mCherry-atb2p and CEN1-GFP at 37°C. Time 0 represents the transition from metaphase to anaphase A, where sister kinetochores are observed to separate to opposite poles. Whereas the metaphase spindle exhibits sustained elongation during the metaphase/anaphase transition in klp6Δ cells, klp6Δ:cut7.24^{ts} cells show transient spindle shrinkage prior to the metaphase/anaphase transition. Scale bar represents 1 μm.

(D) Comparative spindle length versus time plot of klp6Δ (green) and klp6Δ:cut7.24^{ts} (red) cells. Pole-to-pole distance was measured 3.5 min before and 3.5 min after cells exhibited kinetochore separation to opposite poles. At −2 min, the spindle length of the double mutant exhibits a transient shrinkage.

Rescuing Metaphase Spindle Length Rescues Chromosome Segregation Defects Only When Kinetochore-to-MT Attachment Is Not Severely Compromised

The fidelity of chromosome segregation critically depends on the proper kinetochore-to-MT attachment occurring at metaphase [29–32]. There is a correlation between mutations that change the metaphase steady-state spindle length and chromosome segregation defects [19, 34, 35]. We asked whether the apparent rescue of metaphase spindle length seen in the removal of antagonist forces would also rescue chromosome segregation defects. We performed live-cell imaging on mutant strains expressing mCherry-atb2p and CEN1-GFP (marker for the centromere/kinetochore of chromosome 1) [36]. We observed three distinct kinetochore behaviors: normal, where the sister kinetochores separate to opposite poles at anaphase; lagging, where the sister kinetochores are missegregated to one pole but are ultimately corrected and separated to opposite poles; and missegregation, where sister kinetochores stayed at one pole and never separate to opposite poles (Figure 3A). Compared to individual klp5Δ (or klp6Δ), both klp5Δ:ase1Δ and klp6Δ:cut7.24^{ts} showed significant increase in normal kinetochore separation and decrease in lagging or missegregation of chromosome (Figures 3B and 3C). In contrast, compared to individual dam1Δ, dam1Δ:ase1Δ showed no significant change in kinetochore behavior (Figure 3D), while dam1Δ:cut7.24^{ts} showed a decrease in normal kinetochore separation and an increase in kinetochore missegregation (Figure 3E). We conclude that proper kinetochore-to-MT attachment is more important than spindle length regulation for proper chromosome segregation. The artificial minichromosome loss assay also yielded similar conclusions (Figures S3A and S3B).

Transient Spindle Shrinkage Precedes Proper Chromosome Segregation in the klp5Δ:ase1Δ and klp6Δ:cut7.24^{ts} Mutants

How do the klp5Δ:ase1Δ and klp6Δ:cut7.24^{ts} double mutants, which have metaphase spindle lengths similar to wild-type cells, rescue chromosome segregation defects? In live-cell imaging of spindle and kinetochore dynamics, we observed that in all instances where the sister kinetochores were properly separated, approximately 2 min prior to kinetochore separation at anaphase, the spindle length exhibited a transient length decrease before resuming elongation (Figures 4A–4D). The start of resumed elongation coincided with kinetochore separation to opposite poles (Figures 4A–4D). This spindle length decrease only occurs in the double mutants klp5Δ:ase1Δ and klp6Δ:cut7.24^{ts}, but not in the individual mutants klp5Δ or klp6Δ. We conclude that there is a correlation between transient spindle shrinkage and proper chromosome segregation in the klp5Δ:ase1Δ and klp6Δ:cut7.24^{ts} double mutants.

Interestingly, the transient spindle shrinkage prior to kinetochore separation was not observed in dam1Δ, dam1Δ:ase1Δ, or dam1Δ:cut7.24^{ts} mutants (Figures S4A–S4D). This result suggests that the spindle length decrease is not a general mechanism for rescuing chromosome segregation defects. Transient spindle shrinkage, due to instability in the balance of forces, may be a serendipitous mechanism enabling MTs to capture the kinetochores because MT plus ends are now closer to the kinetochores.

In summary, our current study tested the force-balance model in maintaining the steady-state metaphase spindle length in live cells and using a microfluidic temperature-control device to tune on/off temperature-sensitive mutants during mitosis. Although not exhaustive, we chose the key motors and MAPs that individually showed the most drastic changes to spindle length upon their deletion or inactivation. We have defined four categories in relation to force that exemplify the function of the proteins: (1) active outward-force producer (kinesin-5 cut7p), (2) active inward-force transducer (kinesin-8 klp5/6p heterodimer), (3) passive inward-force transducer (kinetochore protein dam1p), and (4) passive inward-force

resistor (MT bundler ase1p). The force balance, or tug-of-war, would be cut7p and ase1p against klp5/6p and dam1p. Clearly, our study is not exhaustive of all spindle proteins. There are hundreds of proteins that contribute to spindle length control [4], and thus our approach of studying simultaneous double deletion or inactivation can be applied systematically to all proteins implicated in metaphase spindle length control to define their individual relative contribution to chromosome segregation defects.

Supplemental Information

Supplemental Information includes four figures, one table, and Supplemental Experimental Procedures and can be found with this article online at http://dx.doi.org/10.1016/j.cub.2013.10.023.

Author Contributions

V.S. and C.F. designed and performed experiments and analyzed data. V.S. and P.T.T. wrote the manuscript.

Acknowledgments

We thank the labs of J.R. McIntosh (University of Colorado), K. Gould (Vanderbilt University), T. Toda (Cancer Research UK), I. Hagan (Paterson Institute Cancer Research), D. McCollum (University of Massachusetts), and Y. Hiraoka (Kansai Advanced Research Center) and the Japan National Bio-Resource Project for generously providing reagents. We thank J. Costa and G. Velve-Casquillas for helpful technical advice and discussion. This work is supported by grants from the National Institutes of Health and Agence Nationale de la Recherche.

Received: April 3, 2013
Revised: August 27, 2013
Accepted: October 9, 2013
Published: November 14, 2013

References

1. Dumont, S., and Mitchison, T.J. (2009). Force and length in the mitotic spindle. Curr. Biol. *19*, R749–R761.
2. Goshima, G., and Scholey, J.M. (2010). Control of mitotic spindle length. Annu. Rev. Cell Dev. Biol. *26*, 21–57.
3. Mogilner, A., and Craig, E. (2010). Towards a quantitative understanding of mitotic spindle assembly and mechanics. J. Cell Sci. *123*, 3435–3445.
4. Goshima, G., Wollman, R., Stuurman, N., Scholey, J.M., and Vale, R.D. (2005). Length control of the metaphase spindle. Curr. Biol. *15*, 1979–1988.
5. Saunders, W.S., and Hoyt, M.A. (1992). Kinesin-related proteins required for structural integrity of the mitotic spindle. Cell *70*, 451–458.
6. Tanenbaum, M.E., Macůrek, L., Janssen, A., Geers, E.F., Alvarez-Fernández, M., and Medema, R.H. (2009). Kif15 cooperates with eg5 to promote bipolar spindle assembly. Curr. Biol. *19*, 1703–1711.
7. Troxell, C.L., Sweezy, M.A., West, R.R., Reed, K.D., Carson, B.D., Pidoux, A.L., Cande, W.Z., and McIntosh, J.R. (2001). pkl1(+)and klp2(+): Two kinesins of the Kar3 subfamily in fission yeast perform different functions in both mitosis and meiosis. Mol. Biol. Cell *12*, 3476–3488.
8. Nabeshima, K., Nakagawa, T., Straight, A.F., Murray, A., Chikashige, Y., Yamashita, Y.M., Hiraoka, Y., and Yanagida, M. (1998). Dynamics of centromeres during metaphase-anaphase transition in fission yeast: Dis1 is implicated in force balance in metaphase bipolar spindle. Mol. Biol. Cell *9*, 3211–3225.
9. Fu, C., Ward, J.J., Loiodice, I., Velve-Casquillas, G., Nedelec, F.J., and Tran, P.T. (2009). Phospho-regulated interaction between kinesin-6 Klp9p and microtubule bundler Ase1p promotes spindle elongation. Dev. Cell *17*, 257–267.
10. Decottignies, A., Zarzov, P., and Nurse, P. (2001). In vivo localisation of fission yeast cyclin-dependent kinase cdc2p and cyclin B cdc13p during mitosis and meiosis. J. Cell Sci. *114*, 2627–2640.
11. Tatebe, H., Goshima, G., Takeda, K., Nakagawa, T., Kinoshita, K., and Yanagida, M. (2001). Fission yeast living mitosis visualized by GFP-tagged gene products. Micron *32*, 67–74.
12. Garcia, M.A., Koonrugsa, N., and Toda, T. (2002). Two kinesin-like Kin I family proteins in fission yeast regulate the establishment of metaphase and the onset of anaphase A. Curr. Biol. *12*, 610–621.
13. West, R.R., Malmstrom, T., and McIntosh, J.R. (2002). Kinesins klp5(+) and klp6(+) are required for normal chromosome movement in mitosis. J. Cell Sci. *115*, 931–940.
14. Erent, M., Drummond, D.R., and Cross, R.A. (2012). S. pombe kinesins-8 promote both nucleation and catastrophe of microtubules. PLoS ONE *7*, e30738.
15. Grissom, P.M., Fiedler, T., Grishchuk, E.L., Nicastro, D., West, R.R., and McIntosh, J.R. (2009). Kinesin-8 from fission yeast: a heterodimeric, plus-end-directed motor that can couple microtubule depolymerization to cargo movement. Mol. Biol. Cell *20*, 963–972.
16. Grishchuk, E.L., Efremov, A.K., Volkov, V.A., Spiridonov, I.S., Gudimchuk, N., Westermann, S., Drubin, D., Barnes, G., McIntosh, J.R., and Ataullakhanov, F.I. (2008). The Dam1 ring binds microtubules strongly enough to be a processive as well as energy-efficient coupler for chromosome motion. Proc. Natl. Acad. Sci. USA *105*, 15423–15428.
17. Grishchuk, E.L., Spiridonov, I.S., Volkov, V.A., Efremov, A., Westermann, S., Drubin, D., Barnes, G., Ataullakhanov, F.I., and McIntosh, J.R. (2008). Different assemblies of the DAM1 complex follow shortening microtubules by distinct mechanisms. Proc. Natl. Acad. Sci. USA *105*, 6918–6923.
18. Loïodice, I., Staub, J., Setty, T.G., Nguyen, N.P., Paoletti, A., and Tran, P.T. (2005). Ase1p organizes antiparallel microtubule arrays during interphase and mitosis in fission yeast. Mol. Biol. Cell *16*, 1756–1768.
19. Yamashita, A., Sato, M., Fujita, A., Yamamoto, M., and Toda, T. (2005). The roles of fission yeast ase1 in mitotic cell division, meiotic nuclear oscillation, and cytokinesis checkpoint signaling. Mol. Biol. Cell *16*, 1378–1395.
20. Subramanian, R., Wilson-Kubalek, E.M., Arthur, C.P., Bick, M.J., Campbell, E.A., Darst, S.A., Milligan, R.A., and Kapoor, T.M. (2010). Insights into antiparallel microtubule crosslinking by PRC1, a conserved nonmotor microtubule binding protein. Cell *142*, 433–443.
21. Grishchuk, E.L., Spiridonov, I.S., and McIntosh, J.R. (2007). Mitotic chromosome biorientation in fission yeast is enhanced by dynein and a minus-end-directed, kinesin-like protein. Mol. Biol. Cell *18*, 2216–2225.
22. Olmsted, Z.T., Riehlman, T.D., Branca, C.N., Colliver, A.G., Cruz, L.O., and Paluh, J.L. (2013). Kinesin-14 Pkl1 targets γ-tubulin for release from the γ-tubuLin ring complex (γ-TuRC). Cell Cycle *12*, 842–848.
23. Hagan, I., and Yanagida, M. (1992). Kinesin-related cut7 protein associates with mitotic and meiotic spindles in fission yeast. Nature *356*, 74–76.
24. Velve Casquillas, G., Fu, C., Le Berre, M., Cramer, J., Meance, S., Plecis, A., Baigl, D., Greffet, J.J., Chen, Y., Piel, M., and Tran, P.T. (2011). Fast microfluidic temperature control for high resolution live cell imaging. Lab Chip *11*, 484–489.
25. Blangy, A., Lane, H.A., d'Hérin, P., Harper, M., Kress, M., and Nigg, E.A. (1995). Phosphorylation by p34cdc2 regulates spindle association of human Eg5, a kinesin-related motor essential for bipolar spindle formation in vivo. Cell *83*, 1159–1169.
26. Kapoor, T.M., Mayer, T.U., Coughlin, M.L., and Mitchison, T.J. (2000). Probing spindle assembly mechanisms with monastrol, a small molecule inhibitor of the mitotic kinesin, Eg5. J. Cell Biol. *150*, 975–988.
27. Saunders, A.M., Powers, J., Strome, S., and Saxton, W.M. (2007). Kinesin-5 acts as a brake in anaphase spindle elongation. Curr. Biol. *17*, R453–R454.
28. Kollu, S., Bakhoum, S.F., and Compton, D.A. (2009). Interplay of microtubule dynamics and sliding during bipolar spindle formation in mammalian cells. Curr. Biol. *19*, 2108–2113.
29. Lara-Gonzalez, P., Westhorpe, F.G., and Taylor, S.S. (2012). The spindle assembly checkpoint. Curr. Biol. *22*, R966–R980.
30. Musacchio, A. (2011). Spindle assembly checkpoint: the third decade. Philos. Trans. R. Soc. Lond. B Biol. Sci. *366*, 3595–3604.
31. Musacchio, A., and Salmon, E.D. (2007). The spindle-assembly checkpoint in space and time. Nat. Rev. Mol. Cell. Biol. *8*, 379–393.
32. Vleugel, M., Hoogendoorn, E., Snel, B., and Kops, G.J. (2012). Evolution and function of the mitotic checkpoint. Dev. Cell *23*, 239–250.

33. Griffiths, K., Masuda, H., Dhut, S., and Toda, T. (2008). Fission yeast dam1-A8 mutant is resistant to and rescued by an anti-microtubule agent. Biochem. Biophys. Res. Commun. *368*, 670–676.
34. Sanchez-Perez, I., Renwick, S.J., Crawley, K., Karig, I., Buck, V., Meadows, J.C., Franco-Sanchez, A., Fleig, U., Toda, T., and Millar, J.B. (2005). The DASH complex and Klp5/Klp6 kinesin coordinate bipolar chromosome attachment in fission yeast. EMBO J. *24*, 2931–2943.
35. West, R.R., Malmstrom, T., Troxell, C.L., and McIntosh, J.R. (2001). Two related kinesins, klp5+ and klp6+, foster microtubule disassembly and are required for meiosis in fission yeast. Mol. Biol. Cell *12*, 3919–3932.
36. Yamamoto, A., and Hiraoka, Y. (2003). Monopolar spindle attachment of sister chromatids is ensured by two distinct mechanisms at the first meiotic division in fission yeast. EMBO J. *22*, 2284–2296.